PROTECT2024

9th International Colloquium on Performance, Protection & Strengthening of Structures Under Extreme Loading & Events

13 - 16 August 2024 I Singapore

CONFERENCE PROCEEDINGS

Organised by

NANYANG TECHNOLOGICAL UNIVERSITY SINGAPORE

NTU CEE Alumni Association

LIST OF TECHNICAL PAPERS

ID Number	Authors (s) – Paper Title
O-4	***Tosei Morita, Daishin Hanaoka, Hiroki Matsumoto*** – Tensile Strength Of Thermoplastic BFRP Rods Simulating Bending Part Under Alkaline Environment
O-6	***Wang Wenming, Hiroki Tamai, Lu Chi, Yoshimi Sonoda*** - Experimental Assessment Ductility Of Reinforced Concrete Pier With Pre- Deformed Reinforcement Under Cyclic Loading

TENSILE STRENGTH OF THERMOPLASTIC BFRP RODS SIMULATING BENDING PART UNDER ALKALINE ENVIRONMENT

Tosei Morita[1], Daishin Hanaoka[2], and Hiroki Matsumoto[3]

[1]Graduate student, Graduate School of Engineering, Kanazawa Institute of Technology, c6300641@st.kanazawa-it.ac.jp.

[2] Professor, Department of Civil and Environmental Engineering, Faculty of Engineering, Kanazawa Institute of Technology, d-hanaoka@neptune.kanazawa-it.ac.jp

[3]Associate Technical Adviser, Innovative Composite Center, Kanazawa Institute of Technology, h-matsumoto@neptune.kanazawa-it.ac.jp

Yatukaho3-1, Hakusan city, Ishikawa state, Japan, 924-0838

Email: c6300641@st.kanazawa-it.ac.jp.

ABSTRACT

Steel bars are used to bear tensile stresses in reinforced concrete (RC) and are used in many structures. However, when the passive film of the rebar is destroyed due to chloride attack or neutralization, corrosion progresses, reducing the durability, as well as the bearing capacity of the structure. A possible solution to this problem is the use of reinforcement with excellent corrosion resistance. For example, Fiber-reinforced plastics (FRP). In order to assess the tensile strength of thermoplastic BFRP (BFRTP), that are composites of basalt fiber and thermoplastic polypropylene, tensile tests of BFRTP rods embedded in cement paste were conducted in an alkaline environment. The results of the test show that the alkaline environment had little effect on the tensile strength of the BFRTP rod if the pH of the cement paste was about 10.98, even if the basalt fiber was exposed.

Keywords: *Thermoplastic BFRP, Basalt fiber, Alkaline environment, Tensile strength.*

1. INTRODUCTION

Figure 1. shows a corrosion of the structure's rebar. Steel bars are used to bear tensile stresses in reinforced concrete (RC) and are used in many structures. If the passive film of the rebar is destroyed by chloride attack or neutralization, corrosion progresses, reducing the durability and the bearing capacity of the structure. One solution to this problem is the use of reinforcement with excellent corrosion resistance.

Fiber-reinforced plastics (FRP) are widely used in various fields because they are lightweight, strong, and do not corrode like steel, and it is expected that in the near future, BFRTP bars will be used in RC structures [1,2]. For this reason, research has been conducted in the use of FRP as reinforcing bars in concrete to extend the service life of structures [3]. The high cost of

thermosetting FRP, which is generally available in the market, is one of the factors that have hindered its widespread use. On the other hand, thermoplastic FRP requires fewer production processes, and if productivity can be improved by continuous molding, cost reduction can be expected [4]. In addition, since FRP rods can easily be molded by applying heat, they are also expected to be used as shear reinforcement. Several investigations of thermosetting FRP used as shear reinforcement have been reported [5,6]. Among those, a study by Maruyama et al [7]. experimentally investigated the tensile strength of CFRP and AFRP in a bent section. Research that while tensile tests on bent steel bars did not fail at corners, FRP failed at both corners, indicating that corner corners are a weak point of FRP. There are only a few studies on thermoplastic FRP, among which Arikawa et al [8] found that even thermoplastic AFRP are weak at corners in bending.

Thermoplastic BFRP (hereinafter referred to as BFRTP, Basalt Fiber Rein-forced Thermo Plastics) is a composite material combining basalt fiber and polypropylene, a thermoplastic resin. Basalt fiber has a superior tensile strength and alkali resistance than glass fiber [9]. The thermoplastic resin (polypropylene) has the characteristic of becoming soft like chocolate when heated and hard when cooled, and since rods are formed with a fiber layer on the inside and a resin on the outside, they have high alkali resistance as reinforcing bars for concrete and can be bent, a characteristic of thermoplasticity. BFRTP rods are expected to be used as stirrups, taking advantage of this characteristic. **Figure 2.** shows the BFRTP rod used in this study. **Figure 3.** shows a BFRTP rod that has undergone the bending process; as it can be seen, the polypropylene resin that forms the rod is damaged in the bent section, exposing the fibers. Exposure to a high alkali environment may cause fiber leaching [10,11].

Therefore, in this study, (1) tensile tests of basalt fibers, (2) tensile tests of BFRTP rods, and (3) tensile tests of BFRTP rods embedded in cement paste were conducted to simulate the bending section of BFRTP rods in an alkaline environment and to determine their tensile strength. In this study, in addition to the strength of basalt fibers in an alkaline environment, we evaluated the tensile strength of BFRTP rods in cement paste. The results of this study contribute to the application of BFRTP rods with bent parts to concrete members and include a great deal of expandability in addition to novelty.

Figure 1. Corrosion of reinforcing steel in the structure

Figure 2. Outline of BFRTP rod

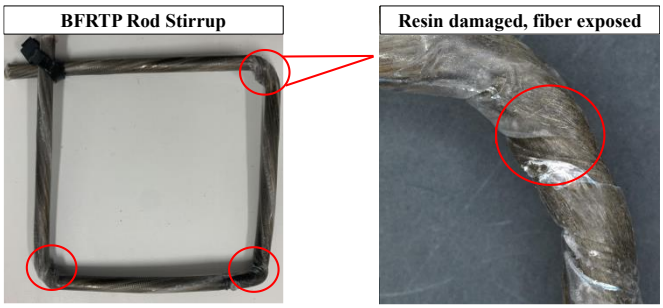

Figure 3. BFRTP rod after bending

2. SINGLE FIBER TENSILE TEST

2.1 Outline of experiment

In this experiment, calcium hydroxide solution (pH 12.8) was used to simulate the alkaline environment in concrete in order to investigate its effect on the Basalt fiber itself**.** Additionally, distilled water (pH7.8) was utilized for a comparison case. Basalt fibers used in BFRTP rods were immersed in calcium hydroxide solution and distilled water for 1, 3, 7, and 28 days (see **Figure 4.**), and tensile tests were conducted on single Basalt fiber threads.

The tensile strength of a single Basalt fiber was determined in accordance with JIS R 7606, as shown in **Figure 5.**

The surface of the Basalt fiber was observed with a microscope and a scanning electron microscope (SEM) to determine the effect of alkaline environment.

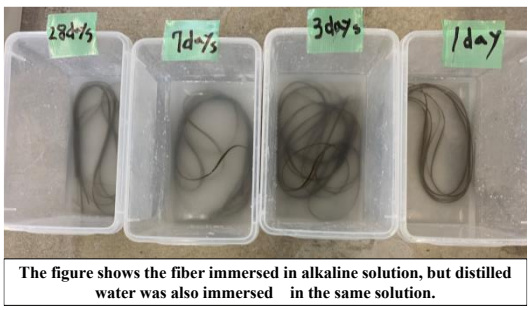

Figure 4. Basalt fiber immersed in alkaline solution

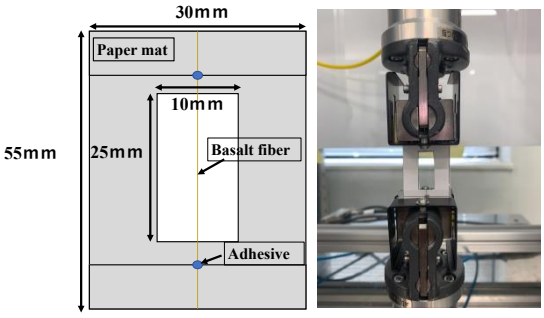

Figure 5. Test specimen overview and tensile

2.2 Results and discussion

Figures 6. and 7. show the change in tensile strength of Basalt fibers due to soaking time, as well as the average value of 20 tests. Basalt fibers soaked in distilled water (pH 7.8) for 1 day showed a 20-30% decrease in strength when compared to sound fibers. However, the tensile strength did not change significantly as the number of soaking days. Basalt fibers soaked in calcium hydroxide solution (pH 12.8) for 1 day showed a 20-50% decrease in strength, similar

to that of distilled water, indicating that the strength decreased with soaking time. No significant change in strength loss was observed in distilled water and alkaline solution due to differences in temperature environment.

In a previous study [10], it was shown that the cross section of glass fiber decreases due to the reaction of SiO_2 in the fiber and NaOH in the alkaline solution. Basalt fibers are also thought to react solution in the same way, resulting in a decrease in fiber cross-section.

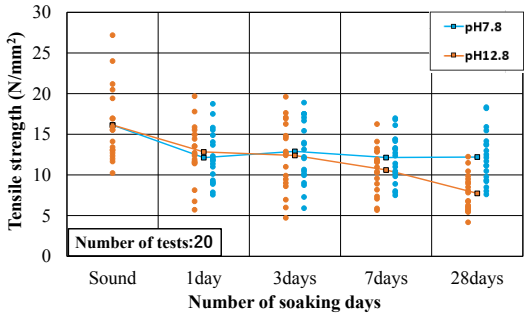

Figures 6. Tensile strength of single thread at 20°C

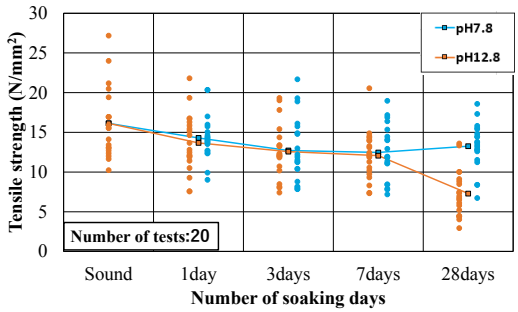

Figures 7. Tensile strength of single thread at 60°C

Figure 8. shows the microscope used and microscopic measurements of the diameters of basalt fibers soaked in pH 12.8 (60°C) for 28 days and healthy fibers at 700x.The average diameter of 10 healthy basalt fibers was 18.89 μm, and the average diameter of 10 basalt fibers immersed in pH 12.8 (60°C) for 28 days was 18.39 μm. These results were unlikely to be due to cross-sectional reduction. Therefore, the surface condition of the Basalt fibers was observed with SEM to investigate the cause of the strength reduction of the fibers.

Figure 9. shows the scanning electron microscope used and a comparison between sound basalt fibers and fibers soaked in pH 7.8, and pH 12.8 at 60°C at 3000x.The surface of the healthy fiber and the basalt fiber soaked at 60°C for 28 days in pH 7.8 are clean, while the basalt fiber soaked at 60°C for 28 days in pH 12.8 is uneven in the area indicated by the red circles. This is due to leaching caused by the alkaline solution. It is thought that this phenomenon occurred in great quantity, leading to a decrease in strength.

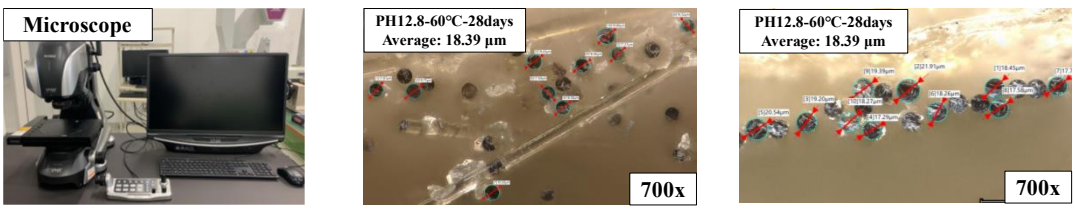

Figure 8. Microscope used and Fiber diameter measurements by microscope (700x)

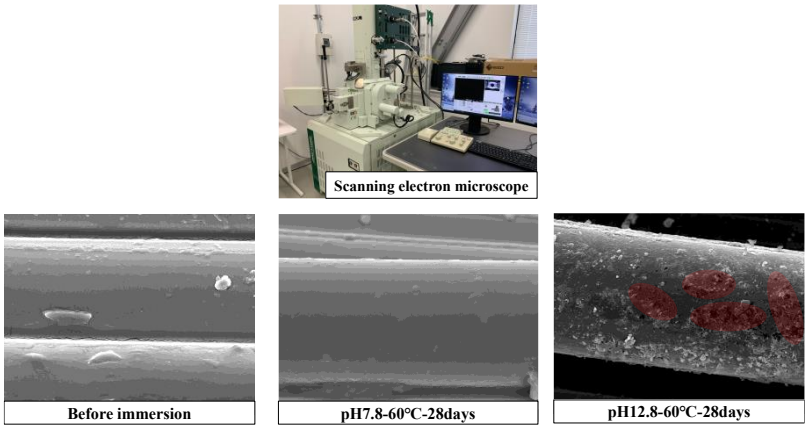

Figure 9. Scanning electron microscope and fiber surface by Scanning electron microscope (3000x)

3. TENSILE TEST OF BFRTP RODS

3.1 Outline of experiment

In this experiment, calcium hydroxide solution (pH 12.8) was once again utilized to simulate the alkaline environment in concrete. Tests were conducted to investigate the effect of the alkaline environment on the tensile strength of BFRTP rods. The experiments considered two cases: (1) sound rods (2) rods with defects (polished with sandpaper). The BFRTP rods were immersed in pH-adjusted solutions of distilled water and calcium hydroxide, and tensile tests were performed after 28 days. To prevent neutralization of the solution during the exposure period, the container was sealed and the exposure was conducted at a room temperature of 20°C.

Figure 10. shows the tensile strength specimens. Threaded steel tubes were attached to both ends of the BFRTP rods after the exposure period was completed, using a static crusher as an expander (Main component: calcium oxide). Tensile tests were conducted at a loading rate of 1.2 N/mm^2/s with a strain gage attached at the center of the specimen. These tests were performed 7 days after placing the expensive agent (total age of the specimens: 35 days) to ensure its sufficient strength.

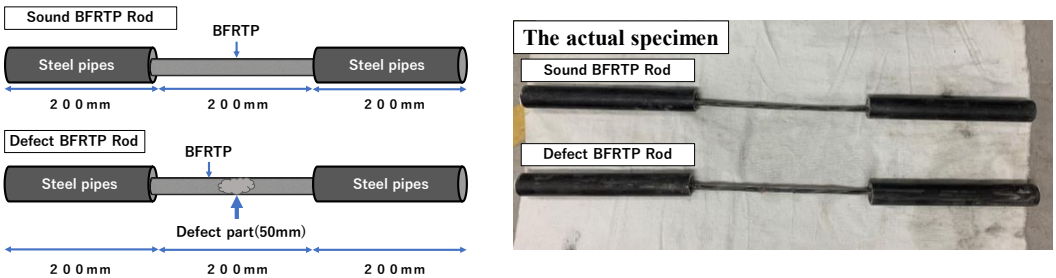

Figure 10. Outline of Tensile Test Specimen

3.2 Results and discussions

Figure 11. presents a stress-strain curve of a BFRTP rod immersed in distilled water (pH 7.8) for 28 days. According to the results, no significant differences were observed between the soundness and rods with defects cases.

Figure 12. present a stress-strain curve of a BFRTP rod immersed in pH 12.8 for 28 days. As it can be observed, there was a decrease in tensile strength in the case of rods with defects. This suggests that exposing fibers to a highly alkaline environment causes a decrease in strength. On the other hand, distilled water did not significantly affect the tensile strength of BFRTP rods with exposed fibers.

Figure 13. shows the average tensile strength of BFRTP rods immersed in alkaline solution for 28 days and the distribution of the data. Although there was some variation in tensile strength, it was not significant for the case of sound BFRTP rods immersed in distilled water and immersed in the alkaline solution. On the other hand, comparing the tensile strength of BFRTP rods with defects immersed in distilled water and immersed in alkaline solution, there was a decrease in strength of about 50 to 150 N/mm^2. This suggests that the alkaline environment degraded the BFRTP rods, resulting in a decrease in strength. The fact that the BFRTP rods with defects showed no reduction in strength in distilled water (pH 7.8) also supports the above conclusion. Although the leaching of fibers and degradation of basalt could not be confirmed visually, test results suggest that BFRTP rods with defects or damage will lose tensile strength when exposed to an alkaline environment.

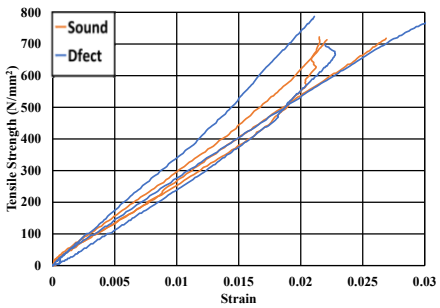

Figure 11. After immersion in pH 7.8 for 28 days

Stress-strain curve of BFRTP

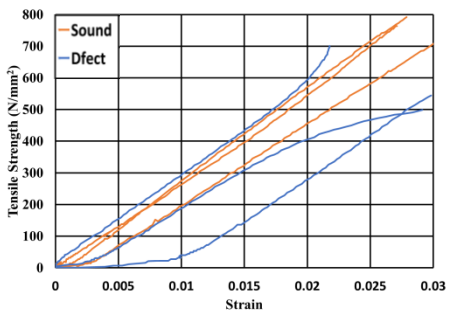

Figure 12. After immersion in pH 12.8 for 28 days

Stress-strain curve of BFRTP

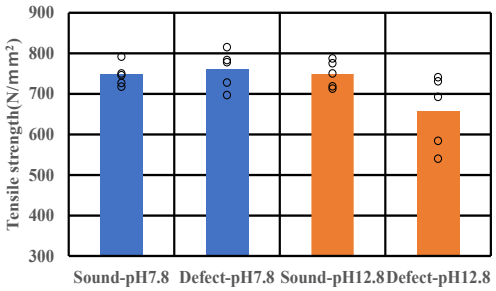

Figure 13. Tensile strength of BFRTP immersed in alkaline solution

4. TENSILE TEST OF BFRTP EMBEDDED IN CEMENT PASTE

4.1 Outline of experiment

Table 1. shows the cement paste composition and compressive strength used in this experiment. It was made of HPC and H+BFS+FA with a water-binder ratio (W/B) of 0.40. The binder was made of high strength Portland cement (H), blast furnace slag fine powder (BFS), and fly ash (FA): 3:5, and the pH was lower than that of the HPC formulation. Here, a soldering trowel was used to melt the resin on the surface of the BFRTP rods to expose the fibers without damaging them. This was done in an area of 50mm of length at the center of the rod. The method utilized in Chapter 3 to case defects on the rods was not utilized in this case as it would also damage the fibers In addition, a case was added in which Polyethylene tape was wrapped around the defective area to prevent alkali solution from penetrating through the defective area was also considered.

Figure 14. presents the tensile test specimens of BFRTP embedded in cement paste. In the experiment, cement paste rectangular prisms of 40 x 40 x 160 mm dimensions were casted at the center of BFRTP rods, wet-cured at 60°C, and after 28 days of age, the BFRTP rods were removed and tensile tests were conducted using the same procedure as described in Chapter 3.

The cement paste pH was also examined using cylindrical specimens. This was done with an electronic pH meter by grinding the specimens until they passed through a 0.15-mm sieve and extracting the filtrate with warm water, in accordance to JIS A 1154, Appendix B.

Table 1. Cement paste mixture

Composition	W/B(%)	Unit weight(kg/m^3)				Compressive strength(N/mm^2)	
		W	H	BFS	FA	7days	28days
HPC	40	552	1380	0	0	75.1	83.5
H＋BFS＋FA			276	414	690	35.9	47.1

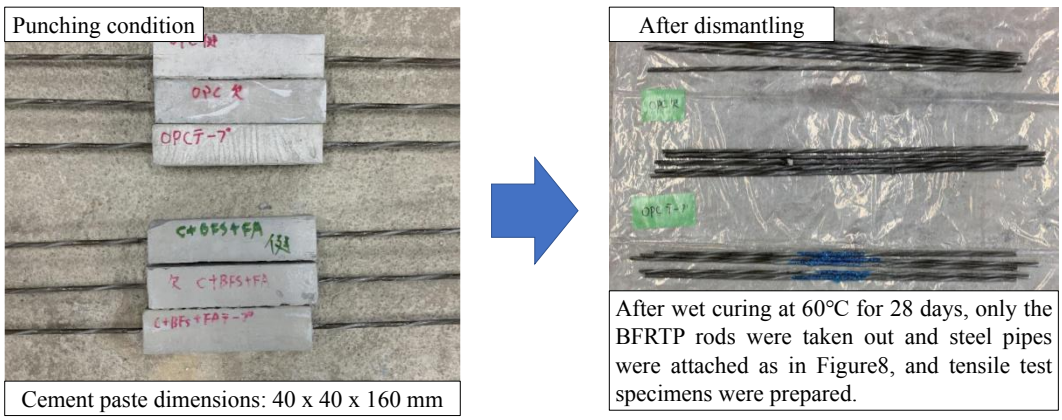

Figure 14. The specimen was embedded in cement paste overview of BFRTP tensile test

4.2 Results and discussions

Figure 15. presents the procedure for measuring the mortar paste, and **Figure 16.** shows the change in mortar paste pH. The results show that the pH of HPC ranged from 13.14 to 11.61 from the fresh condition to 28 days of age, while that of H+BFS+FA ranged from 12.70 to 10.98 in the same time period.

Figure 17. shows the mean tensile strength and variation of the sound and defects BFRTP rods before casting of the paste. A t-test was conducted on these test results to see if there was a significant difference between both of these cases. However, no significant difference was found. Therefore, it is concluded that the method of providing defects utilized in this chapter had little effect on the tensile strength of the BFRTP rods.

Figure 18. shows the mean and variation of the tensile strength of BFRTP rods after being embedded in HPC for 28 days at 60°C. It shows that the tensile strength of the rods did not decrease when they were sound, and that the tensile strength of the rods decreased when the rods were in no good condition. Additionally, there was a strength reduction of about 50% in the case with defects and about 20% in the case of rods of defects + tape. These results suggest that the HPC mortar paste significantly affected the exposed fibers due to its alkaline environment. It is also assumed that utilizing tape reduced the area where the fibers were in contact with the alkali, thereby reducing the strength loss.

Figure 19. shows the average tensile strength of BFRTP rods after being embedded in H+BFS+FA for 28 days at 60°C and their variation. It shows that there was no significant decrease in tensile strength ferny of the considered cases. These results may suggest that the leaching of the fibers has little effect on the tensile strength of the BFRTP rods if the pH of the cement paste is around 10.98, even if the basalt fibers were exposed. However, since the results of this experiment were obtained up to 28 days of age, long-term data is an issue for the future.

The results in this chapter also indicate that the tensile strength of sound BFRTP rods is not affected by the alkaline environment in the concrete because the basalt fibers are protected by the thermoplastic resin and do not exhibit strength loss. On the other hand, the tensile strength of the damaged BFRTP rods was more affected by the alkaline environment of the cement paste than by the alkaline environment of the alkaline solution and showed a decrease in strength. In other words, these results show a similar tendency to the results of the Test specimen overview and tensile shown in Chapter 2, and it is thought that the alkali in the cement paste affects the strength reduction of BFRTP.

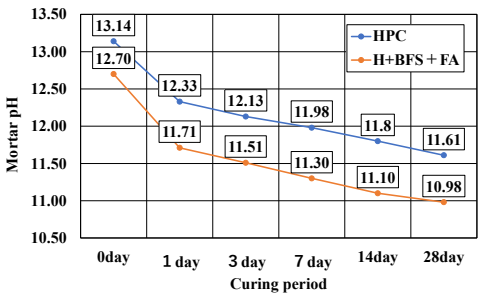

Figure 16. PH of cement paste during curing period

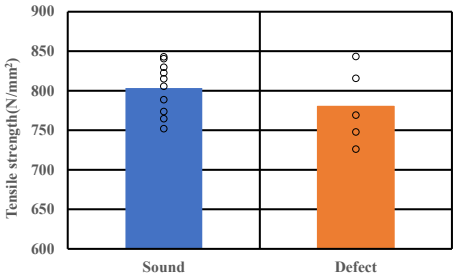

Figure 17. Comparison of soundness and defects of BFRTP rods before casting

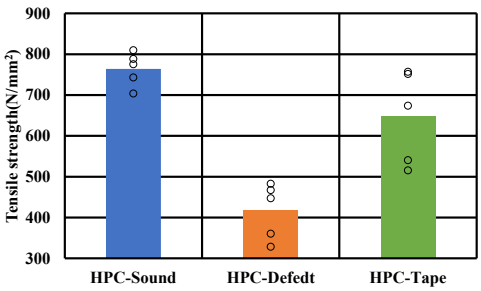

Figure 18. Tensile strength of each HPC case

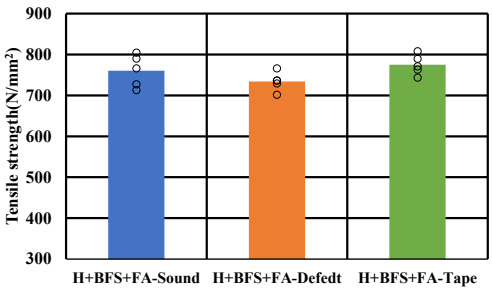

Figure 19. Tensile strength of each H+BFS+FA case

5. Conclusion

The main findings of this study are as follows.

(1) The results of single fiber tests showed that their tensile strength decreased with immersion period under an alkaline solution of pH 12.8. This result was not due to a decrease in the cross-sectional area of the basalt fibers, but was considered to be caused by fiber leaching, to the extent that the surface became uneven, leading to this decrease in strength.

(2) The results indicated that the tensile strength of BFRTP rods with defects or damage decreased when exposed to an alkaline environment with a pH of about 12.8.

(3) The results of tensile tests of BFRTP rods after being embedded in cement paste suggest that the leaching of fibers has little effect on the tensile strength when the pH of the cement paste is around 10.98, even if the basalt fibers are exposed.

ACKNOWLEDGMENT

Some of the results of this research were supported by the 2021 Grant-in-Aid for Scientific Research (Subsidy for Academic Research Fund) Fundamental Research (C 20K04649 Research Director: Daishin Hanaoka).

REFERENCES

[1] Taketo, U. (1990) Application of FRP rods to concrete structures, Production Research, Vol. 44, No. 1, pp. 2-8, 1992.1Borzemski, S. An algorithm for a certain reliability problem. In: *Proc. 7th Int. Conf. on Systems Engineering* (pp. 242-250). Las Vegas, University of Nevada.

[2] Yukihiro, M., & Kunitaro, H. (2018.11). Status of FRP material application in civil engineering and construction, 7th Symposium on FRP Composite Structures and Bridges, pp.68-73.

[3] Hiroshi, M., & Shinya, O., & Hiroaki, N. (2011.11). Fatigue resistance properties of RC floor plate with two types of CFRP reinforcement with different properties, Monthly Report of the Research Institute for Civil Engineering in Cold Region, No.702, pp.2-14,

[4] Shin-ichi, M., & Atsushi, H., & Hisayoshi, U., & Hiroya, T. (2020.1). Application study of thermoplastic FRP to concrete members, Concrete Engineering, Vol.58, No.1, pp.94-98.

[5] Masunobu, C., & Akira S., & Tetsuya, M., & Junichiro, Niwa. (1997.2) Study on Shear Capacity of Concrete Beams Reinforced by Steel Bars and FRP Rods, Journal of JSCE, No.557/V-34, 23-33.

[6] Souji, O., & Makoto, N., & Shuhei, M., & Naohiro Y., & Hiroshi, M., & Kenta, F. (2018.8). Loading Test of RC Structures with Continuous Fiber Reinforcing Bars, 73rd JSCE Annual Conference, V-517, pp.1033-1034.

[7] Takehiko, M., & Masato, Honma., & Hajime, Okamura. (1990) Experimental Study on Tensile Strength of FRP Rods in Bending, Proceedings of the Japan Concrete Institute, Vol.12, No.1, pp.1025-1030.

[8] Naoki, A., & Sumiyuki, M., Nobuhiro, K., & Hiroo, Shinozaki. (2014) Study on Shear Capacity of Beams Reinforced with AFRP Rods Using Thermoplastic Epoxy Resin, Proceedings of the Japan Concrete Institute, Vol.36, No.2.

[9] Kenji Yama, (2021) Forming Process, Vol.33, No.4, pp339-344,

[10] Uomoto, T., & Katsuki, T. (1994) Basic study on evaluation method of alkali resistance of various fibers, Journal of JSCE, No. 490/V-23, pp. 167-174

[11] Kohei, S., & Toru Tanaka, & Tatsu, N., & Koji, I. (2018) A Study on Alkali Resistance of Basalt Short Fiber, Proceedings of the Japan Concrete Institute, Vol.40, No.1, pp339-344.

EXPEIMENTAL ASSESSMENT DUCTILITY OF REINFORCED CONCRETE PIER WITH PRE-DEFORMED REINFORCEMENT UNDER CYCLIC LOADING

Wang Wenming[1], Hiroki Tamai[2], Lu Chi[3], Yoshimi Sonoda[4]

[1] PhD, Kyushu university, wang.wenming.573@s.kyushu-u.ac.jp

[2] Associate Professor, Kyushu university, tamai@doc.kyushu-u.ac.jp

[3] Assistant Professor, Kyushu university, luchi@doc.kyushu-u.ac.jp

[4] Professor, Kyushu university, sonoda@doc.kyushu-u.ac.jp

Corresponding Author: Hiroki Tamai, Associate Professor, Dr.

744 Motooka, Nishi-ku, Fukuoka, JAPAN 819-0395

Email: tamai@doc.kyushu-u.ac.jp

ABSTRACT

To improve the seismic performance of reinforced concrete (RC) members, it is necessary to give sufficient consideration not only to the strength but also to the ductility. In this study, a new ductility improving measure for RC piers was proposed by using longitudinal reinforcement with a pre-deformed inward bending at the plastic hinges. In addition, the full-scale models of RC pier tests were conducted. Lateral cyclic loading experiments for normal specimen and ductility-improving specimen were conducted to investigate the effectiveness of the proposed measure. Their performances were investigated in terms of failure mode, hysteretic properties, and ductility. The results showed that the proposed method could improve the bearing capacity and ductility.

Keywords: *Seismic performance, Ductility, Cyclic loading test, Pre-deformed steel bars, RC pier*

1 INTRODUCTION

The present seismic design methodology for bridges is designed to secure their seismic performance against predetermined design seismic ground motions. However, it does not

inherently ensure performance resilience against seismic events exceeding the designated design assumptions, potentially leading to the failure of bridge components or even the complete collapse of the bridge system. To enhance the overall seismic resilience of the bridge system in the face of larger earthquakes, it becomes imperative to augment both the seismic reinforcement (bearing capacity) and ductility of the bridge components, particularly for the piers. Ductility is the ability of structures to be subjected to several cycle loading and still survive without a substantial strength degradation, and it is necessary for reinforced concrete (RC) structure to avoid all forms brittle failure and provide an early warning of failure without suddenly crush or collapse [1 - 4].

RC pier plays a significant role on seismic performance of concrete structure because it can transmit force from superstructure to the foundations. The stable ability of pier required to resist severe earthquake mainly depends on large inelastic deformations in plastic hinge. There are many methods which focus on enhancing the ductility of RC pier. It is well known that the transverse reinforcement can prevent lateral buckling of the longitudinal reinforcement and confine the core concrete by imposing lateral confining pressure [5 - 8]. Hence, the pier can provide adequate ductility when sufficient transverse reinforcement is provided.

A ductility-improving pier was characterised by placing pre-deformed longitudinal reinforcement in concrete, which could restrict the buckling of the longitudinal reinforcement. The design philosophy was derived from a high-ductility RC beam [9]. As shown in Fig. 1, for normal RC beam, when the concrete failed under compression, the steel bars in compressive area (with a cross-sectional area of about 1/2 to 1/3 that of the steel bars in tensile) would buckle outwards. On this occasion, a balance of forces in the compression and tension zones could not be maintained and the RC beam would collapse. As shown in Fig. 2, the high-ductility beam was installed the longitudinal reinforcement below the compressive damage zone of the concrete [9]. This meant that even if compression damage of concrete occurred, the steel bars would not be easy to buckle. In addition, the forces in the compression and tension zones of the RC beam were balanced, because the longitudinal reinforcements under tension and compression had the same cross-sectional area, as shown in Fig. 2 (c). In brief, force equilibrium could be maintained before and after the failure the concrete on the compression side. The experimental results revealed that the ductility factor was $\mu = 38$.

Based on the methodology described above, to improve the ductility of RC structures, the compressive and tensile forces should be balanced even the compressive failure of concrete occurred. Therefore, as shown in Fig. 3, a RC pier with an improving ductility was designed by pre-deforming the longitudinal reinforcement, which restricted the buckling of longitudinal reinforcement even after the cover was spalled. Hence, the RC pier could still maintain the balance of forces between compressive and tensile steel rebars.

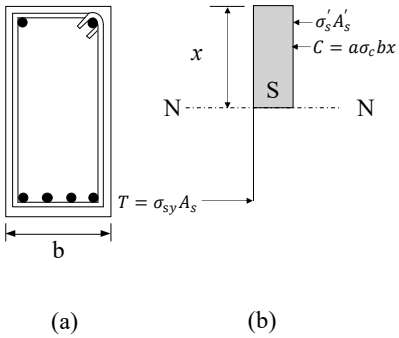

Figure 1. Normal beam: (a) cross section; (b) schematic diagram of the balance of forces.

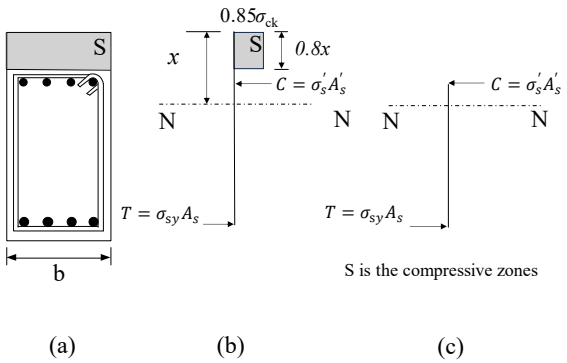

Figure 2. High ductility beam: (a) cross section; (b) schematic diagram of the balance of forces before damage of concrete; (c) schematic diagram of the balance of forces after damage of concrete.

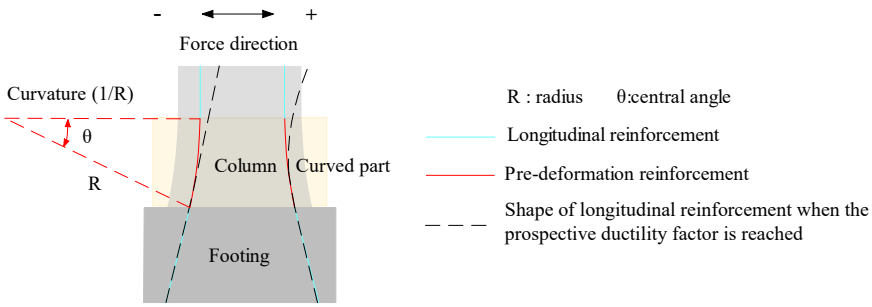

Figure 3. The design philosophy of proposed ductility improvement.

In this paper, the experimental program was conducted to investigate the effect of pre-deformed longitudinal reinforcement on the ductility of RC pier under reversed cyclic load. Tow full-scale model test of normal and ductility-improving piers were conducted by lateral reversed

cyclic load. Their performances were analysis in terms of failure mode, hysteretic properties, and ductility.

2 EXPERIMENTS

2.1 Test specimens

Two RC pier specimens were fabricated for experimentation. The Fig. 4 presented the dimensions and reinforcement layout of test piers. The difference between the two specimens was the shape near the footing. The conventional RC pier, denoted as type 1, served as the referenced specimens. The cross-section was 350 × 300 mm^2 with a height of 1600 mm. While the ductility-improving pier was labelled as type 2. Owing to the curved shape, the dimensions of cross-section for the type 2 partly varied near the footing. The radius of the curved part was 1955 mm. The rest of dimensions of cross-section for type 2 were same as type 1. The cover thickness was maintained 40 mm. The material mechanical parameters of concrete and steel rebars were listed in Table 1 and Table 2.

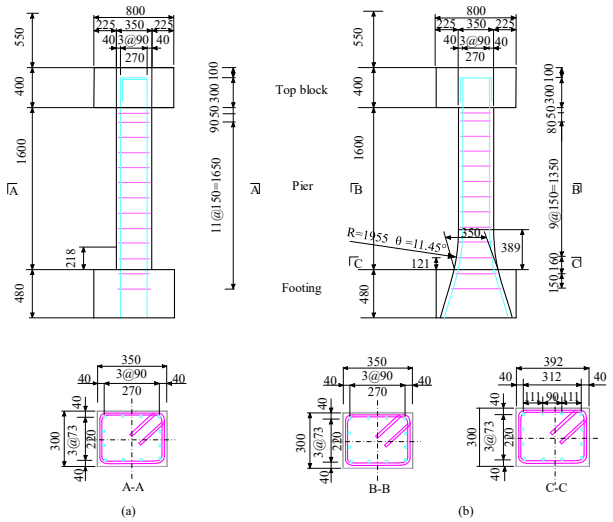

Figure 4. Schematic diagram of reinforcements (a) type 1 (b) type 2

Table 1. Material mechanical parameters of concrete

type 1		type 2	
Compressive strength (N/mm^2)	Tensile strength (N/mm^2)	Compressive strength (N/mm^2)	Tensile strength (N/mm^2)
40.0	3.24	39.4	2.82

Table 2. Material mechanical parameters of steel rebars

Specimens	Yield strength (N/mm^2)	Tensile strength (N/mm^2)	Elongation (%)
Stirrup	388	542	23
Main rebars	404	549	21
Pre-deformed main rebars	400	567	20

2.2 Test procedure

A reversed cyclic displacement-controlled load was applied to the top of specimens as the shown in Fig.5 while the specimens were subjected to constant axial load. Fig. 6 showed the lateral loading history. Three cycles were applied at each displacement level. The initial displacement level was determined to be that when the longitudinal reinforcement reached the initial yield δ_y. The incremental displacement for each cycle was integral multiples of the δ_y, and tests were terminated after the reaction force dropped to below 50% of maximum force F_{max}.

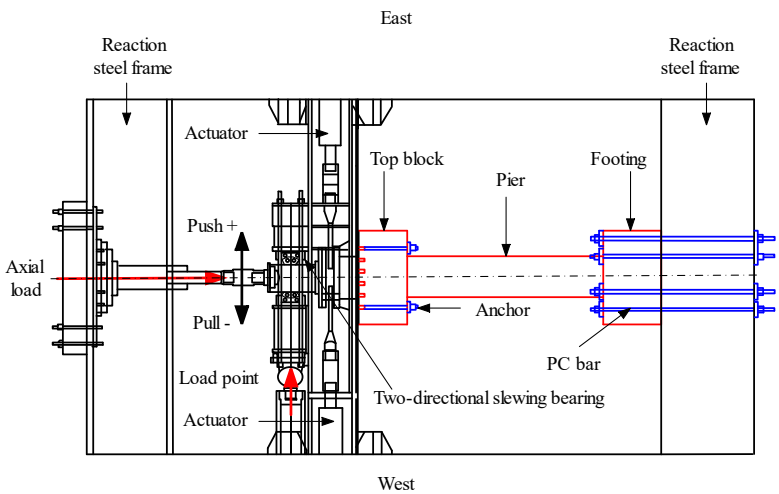

Figure 5. Schematic diagram of setup

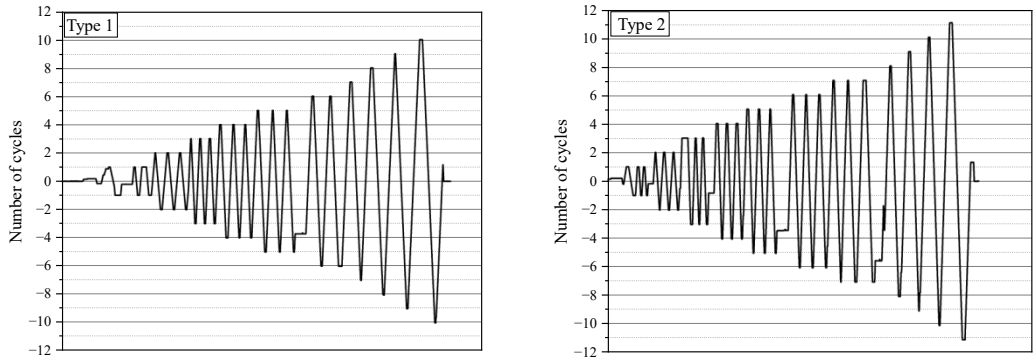

Figure 6. Lateral cyclic loading

3 TEST RESULTS

3.1 Experimental observation

For both samples, the initial cracks appeared in a perpendicular direction to axis of pier. They were distributed around footing. No new main cracks were observed after displacements were $2\delta_y$ and $3\delta_y$ for type 1 and type 2, respectively. The number of cracks and the width of crack developed with the increase of displacement and different cracks connected. Then concrete started spalling and gradually formed plastic damaged area as shown in Fig.7 and Fig. 8. For the type 1 the plastic damaged area manly concentrated near footing. However, for type 2 the plastic damaged area slight moved upward to the top block. The longitudinal reinforcement buckled at a displacement of $9\delta_y$ and $8\delta_y$ for type 1 and type 2, respectively. It was worth mentioning that a buckling in plane for type 1 occurred, but an out plane for type 2, which was not considered during the design phase and buckling in plane was effectively prevented. For both samples, the longitudinal reinforcement failed at $10\delta_y$ with a bending failure.

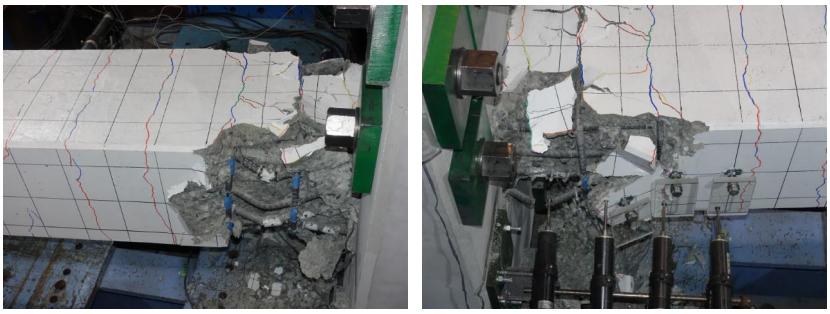

(a) (b)

Figure 7. Failure pattern of type 1: (a) west face; (b) east face.

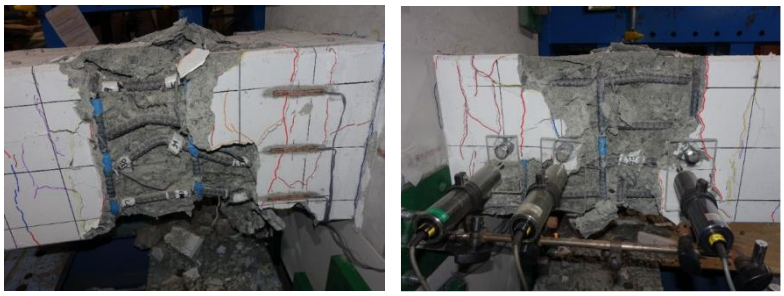

(a) (b)

Figure 8. Failure pattern of type 2: (a) west face; (b) east face

3.2 Hysteresis curves

Fig. 9 showed the comparisons of hysteresis curves between type 1 and type 2. There were stable hysteretic behaviours in type 1 and type 2. The hysteresis curves of type 1 and type 2 were S-shaped and showed a pinching response with the increase of lateral displacement. Meanwhile, the hysteresis curves of type 1 and type 2 were almost centrosymmetric as whole. It indicated that the mechanical properties for both specimens were similar under the reverse cyclic lateral load. The yield displacements δ_y were about 22.5 mm and 18.8 mm for type 1 and type 2, respectively. For type 2, the initial stiffness and bearing were improved due to the increase of cross section. Due to the rupture of longitudinal reinforcement in type 2, the curve abruptly declined down at $10\delta_y$.

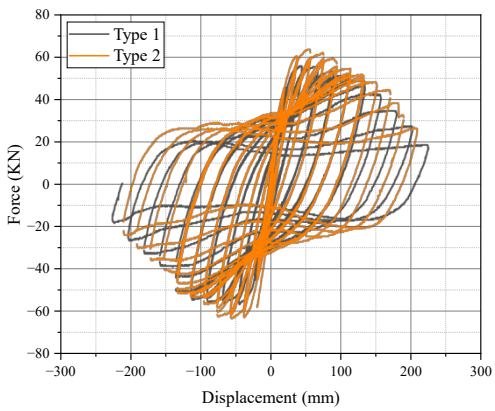

Figure 9. Hysteresis curves of type 1 and type 2.

3.3 Ductility

The ductility referred to a characteristic where the RC pier ranged from yielding to failure. It was usual to quantitatively express ductility by the ductility factor μ, which could be deduced by:

$$\mu = \frac{X_t}{X_y} \tag{1}$$

where X_y was the corresponding displacement of longitudinal reinforcement when first yielding occurred and X_t was the corresponding average ductility displacement when bearing had undergone a 20% reduction, as shown in Fig. 10.

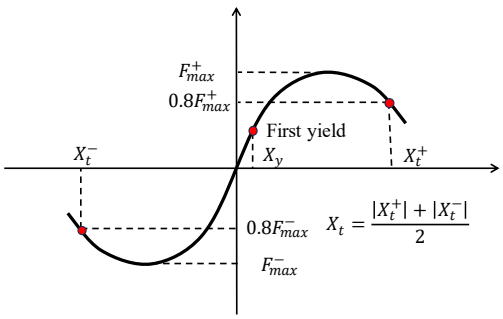

Figure 10. The definition of ductility.

For type 1, the yield displacement δ_y was 22.5 mm, the displacement at maximum load F_{max} was $2\delta_y$ and the test was terminated at $10\delta_y$. However, type 2 had a yield displacement δ_y = 18.8 mm, the displacement at F_{max} was $3\delta_y$ and the test was terminated at $11\delta_y$. The bearing and ductility for each specimen were listed in Table 3. For type 1, the bearing was approximately 54.37 kN. The average ductility displacement was 145.47 mm. The ductility factor μ was derived to be approximately 6.47. Nevertheless, the bearing of type 2 was approximately 62.17 kN. The average ductility displacement was 135.26 mm. The ductility factor μ was 7.19. These results indicated that the bearing and ductility were both enhanced in type 2 due to the pre-deformed longitudinal reinforcements.

Table 3. The ductility parameters for both specimen

Specimen	Bearing (kN)	Ductility displacement (mm)			Yield displacement δ_y (mm)	Ductility factor μ
		Positive	Negative	Average		
type 1	54.37	145.34	-145.61	145.47	22.5	6.47
type 2	62.17	137.61	-132.90	135.26	18.8	7.19

4 CONCLUSIONS

In this paper, a new ductility improving measure for RC piers was proposed by using longitudinal reinforcements, which were inward bending at the plastic hinges. Subsequently, to investigate the effectiveness of the proposed measure, the experiments were conducted on full-scale model of RC piers under cyclic lateral loading. The following main conclusions can be drawn:

As a new measure to improve ductility, this paper proposed a method using inwardly bent longitudinal reinforcement to prevent buckling in plane.

For the type 1 the plastic damaged area manly concentrated near footing. However, for type 2 the plastic damaged area slight moved upward to the top block. For both samples, the longitudinal reinforcement was buckled. For type 1, the buckling occurred in plane. But for type 2, they occurred out plane, which was not assumed at the design stage and buckling in plane was effectively prevented.

The results of the lateral reversed cyclic loading tests showed that the proposed method improved the load bearing capacity and ductility.

ACKNOWLEDGMENTS

This first author is funded by the China Scholarship Council from Ministry of Education of P.R China. (CSC NO. 202107000012).

REFERENCES

[1] Dang, V. H., & François, R. (2014). Prediction of ductility factor of corroded reinforced concrete beams exposed to long term aging in chloride environment. *Cement and Concrete Composites*, 53, 136-147.

[2] Park, R. (1986). Ductile design approach for reinforced concrete frames. *Earthquake spectra*, 2(3), 565-619.

[3] Park, R. (1988, August). Ductility evaluation from laboratory and analytical testing. In: *Proc. 9th world conference on earthquake engineering* (Vol. 8, pp. 605-616). Tokyo-Kyoto Japan.

[4] Sharma, U. K., Bhargava, P., Singh, S. P., & Kaushik, S. K. (2007). Confinement reinforcement design for plain and fibre reinforced high strength concrete columns. *Journal of Advanced Concrete Technology*, 5(1), 113-127.

[5] Yuen, T. Y., Kuang, J. S., & Ho, D. Y. (2017). Ductility design of RC columns. Part 2: extent of critical zone and confinement reinforcement. *HKIE Transactions*, 24(1), 42-53.

[6] Dhakal, R. P., & Su, J. (2018). Design of transverse reinforcement to avoid premature buckling of main bars. Earthquake Engineering & Structural Dynamics, 47(1), 147-168.

[7] Watson, S., Zahn, F. A., & Park, R. (1994). Confining reinforcement for concrete columns. Journal of Structural Engineering, 120(6), 1798-1824.

[8] Anzlin, A., Fischinger, M., & Isakovic, T. (2015). Cyclic response of I-shaped bridge columns with substandard transverse reinforcement. Engineering Structures, 99, 642-652.

[9] Masami Koshiishi. (2017). High-ductility RC beam structure. Japan Patent No. 6152975.

PROTECT2024